

Terahertz-Induced Oscillations in Encapsulated Graphene

Jesús Iñarrea* and Gloria Platero

A theoretical study on the rise of photo-oscillations in the magnetoresistance of hexagonal boron nitride (hBN)-encapsulated graphene is presented. The previous radiation-driven electron orbit model devised to study the same oscillations, well-known as MIRO, in 2D semiconductor systems (GaAs/AlGaAs heterostructure) is used. It is obtained that these graphene platforms under radiation and a static magnetic field are sensitive to terahertz and far-infrared radiation. The power, temperature, and frequency dependences of the photo-oscillations are studied. For power dependence, it is predicted that for cleaner graphene and high enough power it is possible to observe zero-resistance states and a resonance peak.

1. Introduction

Microwave-induced magnetoresistance (R_{xx}) oscillation (MIRO)^[1,2] is a remarkable effect that along with zero-resistance states (ZRS) surprised the condensed matter community when they were discovered.^[3–5] ZRS are obtained from MIRO when radiation power is sufficiently increased.

Many experiments^[6–22] and theoretical^[23–39] works have been carried out so far, but the physical origin is still under question. Yet, we can claim that MIRO represents a universal effect that shows up in different 2D platforms and a novel demonstration of radiation–matter interaction. Thus, we can consider that under which conditions graphene^[40] could be a feasible candidate to support radiation-induced resistance oscillations. A pioneering theoretical work has been recently published predicting the rise of radiation-induced resistance oscillations in monolayer and bilayer graphene.^[41] Likewise, a remarkable experimental work^[42] using

hBN-encapsulated graphene has been published showing similar oscillations to MIRO but in the terahertz band. Another theoretical work has been published^[43] trying to explain the experiment^[42] with an extension of the radiation-driven electron orbit model previously used for MIRO in 2D GaAs systems.^[23,24]

In this article, we theoretically study the rise of MIRO in hBN-encapsulated monolayer graphene systems presenting an extension of the irradiated graphene model and further results not shown in the previous work.^[43] Monolayer graphene


over a substrate or encapsulated is considered as a gapped system and the Dirac fermions formerly massless become massive.^[44–49] This condition is more pronounced when a vertical electric field is applied to the system (gated graphene). hBN-encapsulated graphene presents one of the highest mobilities ($\mu = 3 \times 10^5 \text{ cm}^2 \text{ Vs}^{-1}$) in graphene systems. High mobility which implies a cleaner system is key to observe MIRO. In our approach we use the theoretical model of radiation-driven electron orbits^[23,24] and apply it to massive Dirac fermions to study the appearance of photo-oscillations in the magnetoresistance of hBN-sandwiched graphene.

In our calculations we first obtain that the oscillations are mainly sensitive to terahertz radiation and thus, we are dealing with terahertz-induced resistance oscillations (TIRO); far-infrared frequencies can be reached too. In regard to the previous work, we present novel results in terms of the tunable bandgap (new effective masses) introducing the equivalence to the 2D electron density for a better comparison with experiment.^[42] In the same way, we further study the dependence of TIRO on radiation power (P) presenting the results in terms of R_{xx} versus B for a different effective mass and all the curves for different P in the same figure. The results show a clear oscillation quenching for a decreasing P ; meanwhile, the Shubnikov de Haas oscillations are hardly affected. We predict that with better graphene samples (higher mobility) and with high enough power it would be possible to obtain simultaneously two important effects, zero-resistance states in graphene and a resonance peak very close to the resonance condition $\omega = \omega_c$, where ω is the radiation frequency and ω_c the cyclotron frequency. According to our simulations, for such higher P , the ZRS region will increasingly broaden and the resonance peak will get very acute. The important point is that this resonance peak will never be centered on the exact resonance point of $\omega = \omega_c$. In the case of temperature (T), we present results for a lower effective mass (not shown before) and similarly to P we show them with R_{xx} versus B . In this way, we are able to observe simultaneously the variation with T of both TIRO and Shubnikov de Haas oscillations. Thus, we observe a clear decreasing of TIRO oscillations with increasing T but much slower when

J. Iñarrea
Escuela Politécnica Superior
Universidad Carlos III
Leganes, 28911 Madrid, Spain
E-mail: jinarrea@fis.uc3m.es

J. Iñarrea, G. Platero
Instituto de Ciencia de Materiales
CSIC
Cantoblanco, Madrid 28049, Spain

G. Platero
Unidad Asociada al Instituto de Ciencia de Materiales
CSIC
Cantoblanco, Madrid 28049, Spain

 The ORCID identification number(s) for the author(s) of this article can be found under <https://doi.org/10.1002/pssb.202200266>.

© 2022 The Authors. physica status solidi (b) basic solid state physics published by Wiley-VCH GmbH. This is an open access article under the terms of the Creative Commons Attribution License, which permits use, distribution and reproduction in any medium, provided the original work is properly cited.

DOI: 10.1002/pssb.202200266

compared with MIRO in GaAs platforms. The latter disappear in a few degrees. In the case of Shubnikov de Haas oscillations, they disappear in a similar rate as in the case of GaAs platforms, that is, much faster than TIRO oscillations. The most important and surprising result is that TIRO persist at much higher T reaching around 200 K. In our simulations (not shown) we reach room temperature when using cleaner samples and higher radiation frequencies. Finally we study the dependence on frequency showing new results with higher frequencies in regard to the previous work.^[43] These novel results are presented as in the cases of P and T as R_{xx} versus B . Thus, we observe in a more direct way how the oscillations get lower as the frequency increases, specially at higher frequencies (1.5 and 2.0 THz). Nevertheless, the Shubnikov de Haas oscillations remain hardly unaffected by the frequency change.

2. Theoretical Model

The theoretical model to study irradiated resistance oscillations in monolayer graphene is based in two main parts. The first part considers gapped monolayer graphene. It is well known that graphene on top of the substrate becomes gapped because the carbon sublattice symmetry is broken.^[50,51] Thus, monolayer graphene becomes a semiconductor and, what is more important for our model, the carriers (Dirac fermions) become massive. The theory of gapped monolayer graphene is already developed.^[52,53] Thus, the Hamiltonian of gapped graphene with a perpendicular magnetic field $\vec{B} = (0, 0, B)$, at the K point, is given by

$$H_K = \begin{pmatrix} \Delta & v_F \pi_- \\ v_F \pi_+ & -\Delta \end{pmatrix} \quad (1)$$

$v_F \simeq 1 \times 10^6 \text{ m s}^{-1}$ is the Fermi velocity, $\pi_{\pm} = \pi_x \pm i\pi_y$, $\pi_x = P_x$, and $\pi_y = P_y + eBx$, where we have used the Landau gauge, $\vec{A} = (0, Bx, 0)$. Δ is a massive term. The eigenenergies and eigenfunctions,^[52,53] for the K valley

$$E_{n,K} = \pm \sqrt{(\hbar w_B)^2 |n| + \Delta^2}; \quad (n = \pm 1, \pm 2, \dots) \quad (2)$$

$$E_{0,K} = -\Delta \quad (3)$$

for the energies and

$$\Phi_{n,K} \propto \begin{pmatrix} \phi_{|n|-1} \left(x + \frac{\hbar k_y}{eB} \right) \\ \phi_{|n|} \left(x + \frac{\hbar k_y}{eB} \right) \end{pmatrix} \quad (4)$$

for the eigenstates, where ϕ_n is the standard Landau level wavefunction and $w_B = v_F \sqrt{2}/l_B$, l_B being the magnetic length.

Following the theory by Koshino,^[52,53] we can expand the Hamiltonian near the conduction band bottom and obtain an effective expression for the Hamiltonian at the K valley.^[52]

$$H_K \simeq \frac{v_F^2}{2\Delta} \pi_- \pi_+ = \frac{\pi^2}{2m^*} - \frac{\hbar w_c}{2} \quad (5)$$

The cyclotron frequency w_c is given by $w_c = eB/m^*$, m^* being the effective mass of the massive Dirac fermions

$$m^* = \frac{\Delta}{v_F^2} \quad (6)$$

Thus, m^* turns out to be gap dependent and can be tuned, for instance, by an external bias. We can write a more developed expression for the effective Hamiltonian $H_{K/K'}$

$$\left[\frac{P_x^2}{2m^*} + \frac{(P_y^2 + eBx)}{2m^*} \mp \frac{1}{2} \hbar w_c \right] \Phi_{n,K/K'} = E_{n,K/K'} \Phi_{n,K/K'} \quad (7)$$

which is the Schrödinger equation in the presence of a static B and the corresponding eigenfunctions in a stationary scenario are Landau states. ‘-’ sign would correspond to K and ‘+’ to K' .

Now the second part of the theoretical model comes into play and we apply the radiation-driven electron orbit model that was previously developed^[23,36,54–57] to deal with MIRO, to the above effective Hamiltonian adding a time dependent term (radiation) and a DC electric field in the x -direction

$$H(t) = \frac{P_x^2}{2m^*} + \frac{1}{2} m^* w_c^2 (x - X)^2 - eE_{dc} X + \frac{1}{2} m^* \frac{E_{dc}^2}{B^2} - eE_0 x \cos wt \quad (8)$$

E_{dc} is the driving DC electric field responsible for current, X is the center of the Landau state orbit: $X = -\frac{\hbar k_y}{eB} + \frac{eE_{dc}}{m^* w_c^2}$, and E_0 the intensity of the radiation field. $H(t)$ can be exactly solved allowing a solution for the massive Dirac fermion wave function (for the K valley)

$$\Phi_{n,K} \propto \begin{pmatrix} \phi_{|n|-1} \left(x + \frac{\hbar k_y}{eB} - x_{cl}(t), t \right) \\ \approx 0 \end{pmatrix} \quad (9)$$

The time-dependent guiding center shift $x_{cl}(t)$ is given by

$$x_{cl}(t) = \frac{e^{-\gamma t/2} e E_0}{m^* \sqrt{(w_c^2 - w^2)^2 + \gamma^4}} \sin wt = A(t) \sin wt \quad (10)$$

One important result of the radiation-driven electron orbit model is that the Landau states perform a classical harmonic motion driven by radiation and according to $x_{cl}(t)$.

In this swinging motion, electrons interact with different sources of disorder, such as lattice ions, defects in general (graphene wrinkles and corrugations), and the sample edges giving rise to a process of oscillations quenching or damping. The damping is phenomenologically introduced through the γ -dependent damping term in the previous $x_{cl}(t)$ equation. The phenomenological equation to express γ ^[43,58] is given by, $\gamma = a + b(T)$, a being an average frequency term representing the driven Landau states oscillations and accordingly proportional to the radiation frequency. Thus, if we are dealing with THz radiation, $a = 10^{12} \text{ s}^{-1}$. $b(T)$ is the electron scattering rate with acoustic phonons and it depends linearly with T ^[59–61] according to $b(T) = 1/\tau_{ac} \simeq (10^{11} - 10^{12}) \times T \text{ s}^{-1}$ for monolayer graphene.

To calculate magnetoresistance (R_{xx}) we consider the long-range Coulomb disorder (charged impurities) as the main source

of scattering.^[59] Based on a semiclassical Boltzmann transport theory, we calculate first the average distance advance by the carriers in a scattering jump, ΔX .^[23,24,62–65] ΔX is at the heart of the irradiated magnetoresistance oscillations. The final expression for the irradiated ΔX is given by^[36,66]

$$\Delta X = \Delta X(0) - A \sin\left(2\pi \frac{w}{w_c}\right) \quad (11)$$

where $\Delta X(0)$ is the distance between the guiding centers of the final and initial Landau states in the dark. Next we calculate the longitudinal conductivity, σ_{xx} .^[54,59,65–68]

$$\sigma_{xx} = 2e^2 \int_0^\infty dE \rho_i(E) (\Delta X)^2 W_1 \left(-\frac{df(E)}{dE}\right) \quad (12)$$

F being the energy, $\rho_i(E)$ the density of initial Landau states, and $f(E)$ the Fermi distribution function. W_1 is the scattering rate of electrons with charged impurities.

To obtain R_{xx} , we use the standard tensorial relation $R_{xx} = \frac{\sigma_{xx}}{\sigma_{xx} + \sigma_{xy}}$, where $\sigma_{xy} \simeq \frac{n_i e}{B}$, n_i is the electron density, and e the electron charge.

3. Results

In **Figure 1** we exhibit calculated magnetoresistance under radiation versus B . The radiation frequency is 700 GHz and

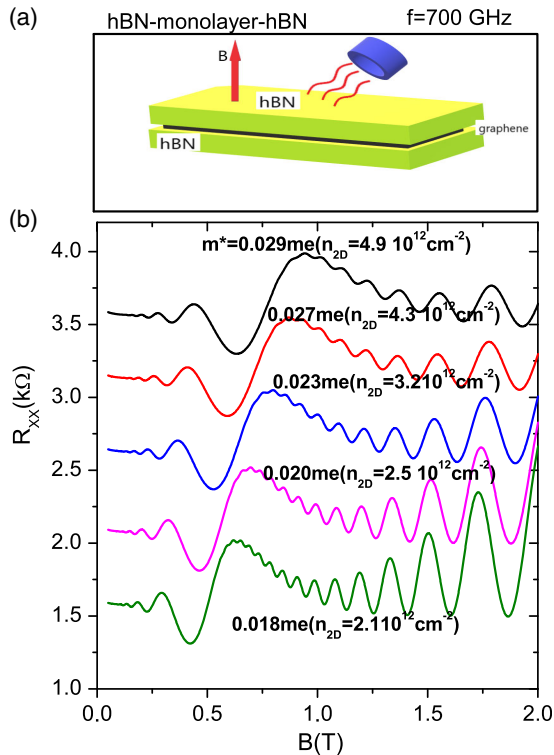


Figure 1. a) Schematic diagram of the basic experimental set up: irradiated hBN-sandwiched monolayer graphene under B . b) Calculated magnetoresistance under radiation versus B . The radiation frequency is 700 GHz. We present five curves that correspond to five different external electric fields that in turn correspond to five effective masses from $m^* = 0.018 m_e$ to $0.029 m_e$. $T = 1$ K and $P = 2$ mW.

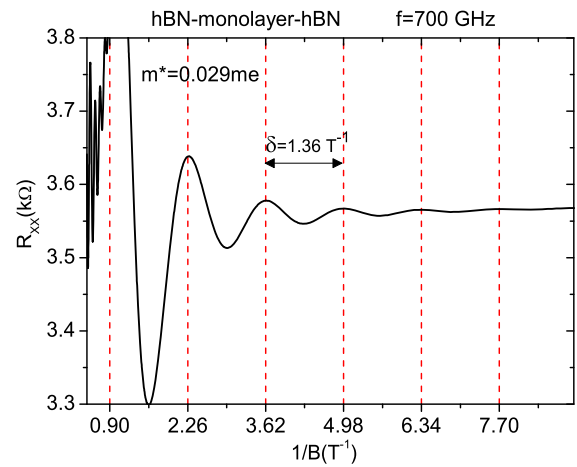


Figure 2. a) Calculated magnetoresistance under radiation versus the inverse of B . The radiation frequency is 700 GHz. We exhibit the case of $m^* = 0.029 m_e$. We present one of the main characteristics of MIRO: oscillations are periodic in the inverse of B . In this case the period is $\delta = 1.36 T^{-1}$. $T = 1$ K and $P = 2$ mW.

$T = 1.0$ K. The upper panel (**Figure 2a**) shows the basic experimental setting: hBN-sandwiched monolayer graphene under light and B . We present five curves corresponding to five effective masses (external bias) in increasing order beginning from $0.018 m_e$ up to $0.029 m_e$. Certainly every effective mass corresponds in time to a different bandgap. Two main system parameters can be tuned simultaneously by the external bias. One is the bandgap^[69] and the other is the position of the Fermi energy, that is, the 2D massive Dirac Fermions density n_{2D} . For this reason and to contrast with experiment, every curve label presents two numerical values: the effective mass and the carrier density. Based on a previous work,^[69] the external bias we have used in the simulations ranges from 0.30 to 0.90 V \AA^{-1} that corresponds to bandgaps from 210 to 320 meV. Thus, the effective masses range from 0.018 to $0.029 m_e$. In the same way, we can obtain approximate values for n_{2D} from the vertical electric field between the two outer layers of hBN (E_{\perp}). Our calculations, based on basic electrostatics, yields a charge density $n_{2D} = \frac{\epsilon E_{\perp}}{e}$, that goes from 0.5×10^{12} to $5 \times 10^{12} \text{ cm}^{-2}$. These calculated n_{2D} are in qualitative agreement with the ones used in the experiment.^[42]

In **Figure 2**, we present calculated magnetoresistance under radiation versus the inverse of B . The frequency is 700 GHz and $T = 1$ K. In this figure, we can check one of the main features of photo-oscillations. The red vertical lines mark the peaks of the oscillations and the distance between them is constant (period). Thus, TIRO are periodic with $1/B$. This is expected from the theoretical model and agrees with the experimental results^[42] and with the previous results obtained with MIRO in semiconductor platforms.^[1]

In **Figure 3** we present calculated magnetoresistance under radiation versus B for different radiation powers. The radiation frequency is 700 GHz. We present the irradiated magnetoresistance versus B for a decreasing radiation intensity from the highest power to the dark. Seven irradiated curves are exhibited, showing that the oscillations dim as the radiation power lowers.

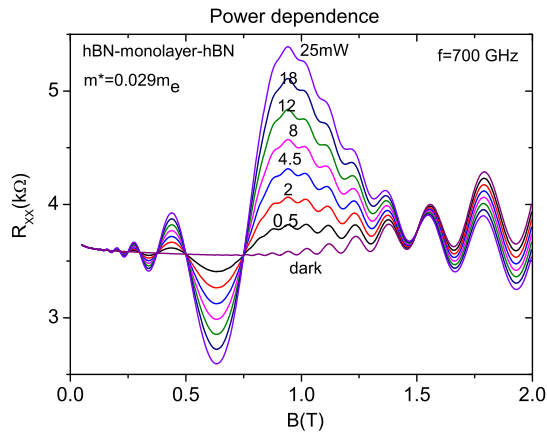


Figure 3. Calculated magnetoresistance versus B for different radiation powers, a radiation frequency of 700 GHz and an effective mass of $m^* = 0.029 m_e$. Seven curves of irradiated magnetoresistance and the dark case versus B is exhibited. The oscillations clearly dim from the highest power to the dark. The simulations indicate an attenuation rate according to a sublinear relation (square root). $T = 1$ K.

The power values are: 25, 18, 12, 8, 4.5, 2, and 0.5 mW. Our simulations show that the variation of R_{xx} with P suggests a sublinear relation such as: $\Delta R_{xx} \propto P^{0.5}$. As expected, this result is in agreement with our model and resembles the experimental one.^[42]

In **Figure 4** we present the variation with temperature of TIRO in hBN-sandwiched graphene. We exhibit 12 irradiated magnetoresistance curves versus B for 12 different T . It can be observed again that the oscillations progressively dim as T increases from 1 K up to 200 K. The Shubnikov de Haas oscillations are wiped out in just a few degrees and at 10 K they can hardly be seen. However TIRO persists at much higher T and can still be observed at temperatures close to 200 K. Thus one interesting point rises in the sense that with cleaner and more perfect graphene samples it would be possible in experiments to observe TIRO at room T . We have run simulations at higher frequencies

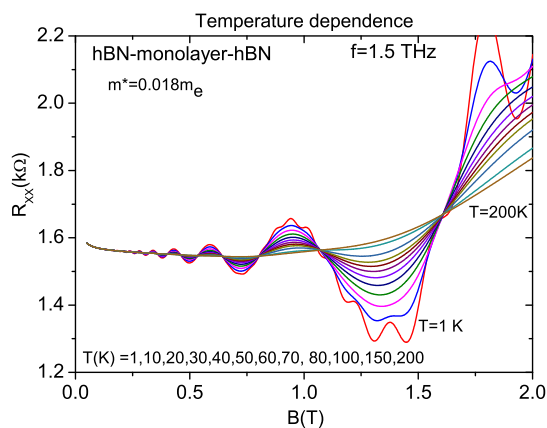


Figure 4. Temperature dependence of TIRO. 12 irradiated magnetoresistance curves versus B are exhibited for twelve different T . It can be observed that the photo-oscillations progressively disappear as T increases from 1 K up to 200 K. The Shubnikov de Haas oscillations disappear at low T and at 10 K they can hardly be seen; however, TIRO remains much longer. $P = 2$ mW.

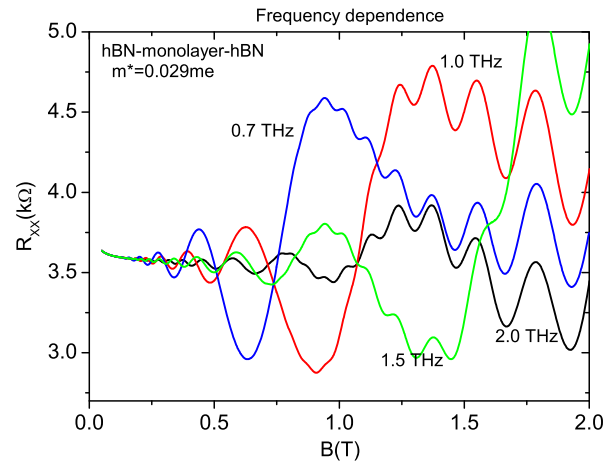


Figure 5. Calculated magnetoresistance versus B for four different frequencies: 700 GHz, 1.0 THz, 1.5 THz, and 2.0 THz. It can be observed that as frequency rises the number of magnetoresistance oscillations increases too but the amplitude dims. $T = 1$ K and $P = 8$ mW.

and lower damping factor and the results (not shown in this article) indicate that TIRO at room T is a feasible scenario. The calculated results are qualitatively similar to experiment.^[42]

In **Figure 5** we present the calculated results on the variation of irradiated magnetoresistance versus B of the sandwiched graphene with radiation frequency. We present four curves of different frequencies. The frequencies are 700 GHz, 1.0 THz, 1.5 THz, and 2.0 THz. The latter can be considered as far infrared. We obtain more oscillations but smaller amplitudes for higher frequencies. More simulations with larger frequencies (not shown) have been run confirming this trend. As in the previous figures, the results are similar to the ones obtained in experiments.^[42] However, in the frequency case, the attenuation rate for the oscillations is slower in the calculated cases than in experiments.^[42]

In **Figure 6**, we study the variation of the ZRS region and resonance peak with frequency and effective mass. Thus, we exhibit the calculated magnetoresistance under radiation versus B for frequencies of 700 GHz and 1 THz and effective masses of 0.029 and 0.018 m_e . For all cases we obtain ZRS and resonance peaks for high radiation power. The interesting point is that all resonance peaks turn out to be asymmetric and never reach the resonance value of $\omega = \omega_c$. The reason is the existence of the sine term in the expression of the irradiated magnetoresistance that equals zero when $\omega = \omega_c$. At the same time the denominator of the amplitude, A , approaches 0 too and the amplitude increases abruptly. Both situations coincide when $\omega = \omega_c$. Interestingly enough, this situation contrasts with other resonance situations, where the corresponding resonance peak shows up as well centered and symmetric.

4. Conclusion

Summarizing, we have presented a theoretical study on the rise of radiation-induced oscillations in hBN-encapsulated graphene. The study is motivated by recent experimental results^[42] on the

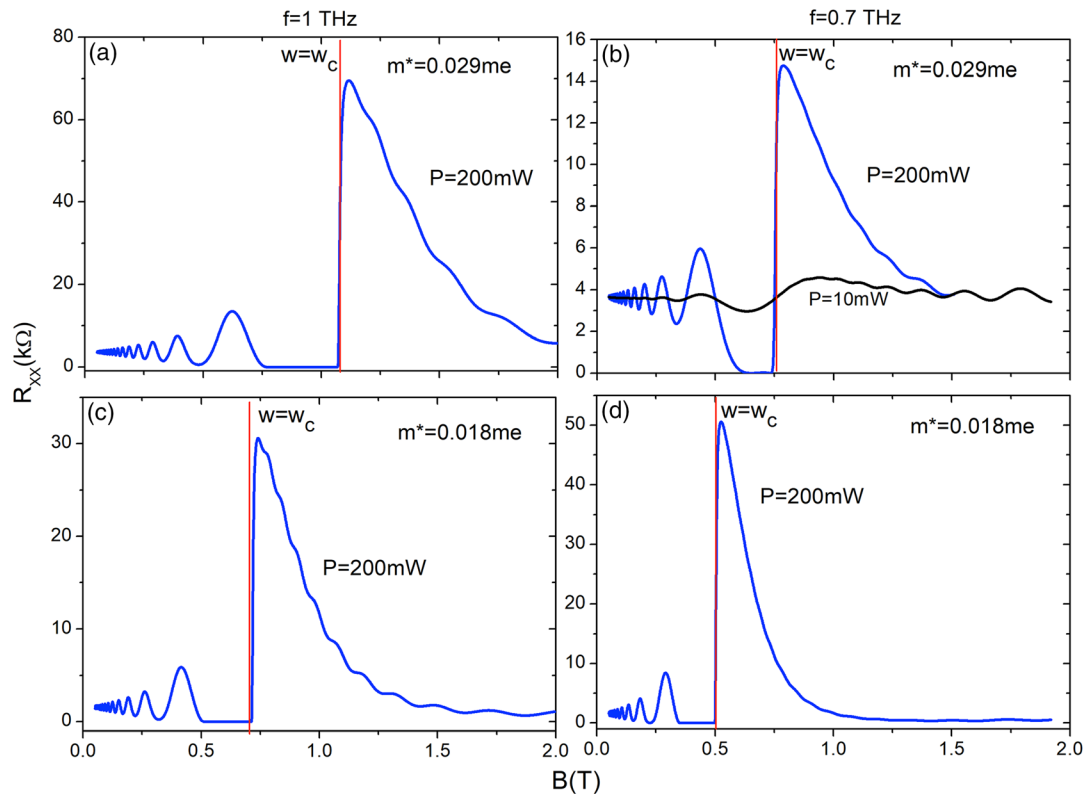


Figure 6. Variation of the ZRS region and resonance peak with frequency and effective mass. We exhibit the calculated magnetoresistance under radiation versus B for frequencies of 700 GHz and 1 THz and effective masses of 0.029 and 0.018 m_e . In all cases the asymmetric resonance peaks never reach the resonance value of $\omega = \omega_c$. $T = 1$ K.

appearance of photo-oscillations in this graphene platform. We have studied the dependence with the external bias in a gated scenario. The bias tunes the Fermi-level position and the Dirac fermion effective mass. First, we have obtained that the oscillations mainly show up or are sensitive to terahertz radiation. We have studied the oscillation dependence with radiation power, temperatures, and frequency. Interestingly enough, we have predicted that for cleaner graphene samples it would be possible to observe radiation-induced oscillations at room temperature. In the same way for very high radiation power, it would be possible to reach ZRS and something similar to a resonance peak close to $\omega = \omega_c$ but not in the right resonance position.

Acknowledgements

This work is supported by the MINECO (Spain) under grant PID2020-117787GB-I00 and by the Madrid Government (Comunidad de Madrid-Spain) under the Multiannual Agreement with UC3M in the line of Excellence of University Professors (EPUC3M14), and in the context of the V PRICIT (Regional Programme of Research and Technological Innovation). We also acknowledge the CSIC Research Platform on Quantum Technologies PTI-001.

Conflict of Interest

The authors declare no conflict of interest.

Data Availability Statement

The data that support the findings of this study are available from the corresponding author upon reasonable request.

Keywords

hBN-encapsulated graphene, magnetoresistance, terahertz-induced oscillations

Received: June 17, 2022

Revised: August 25, 2022

Published online: September 13, 2022

- [1] R. G. Mani, J. H. Smet, K. von Klitzing, V. Narayanamurti, W. B. Johnson, V. Umansky, *Nature* **2002**, 420, 646.
- [2] M. A. Zudov, R. R. Du, L. N. Pfeiffer, K. W. West, *Phys. Rev. Lett.* **2003**, 90, 046807.
- [3] J. Iñarrea, G. Platero, *Phys. Status Solidi A* **2006**, 203, 1148.
- [4] J. Iñarrea, R. Aguado, G. Platero, *Europhys. Lett.* **1997**, 40, 417.
- [5] J. Iñarrea, G. Platero, *Europhys. Lett.* **1996**, 34, 43.
- [6] R. G. Mani, J. H. Smet, K. von Klitzing, V. Narayanamurti, W. B. Johnson, V. Umansky, *Phys. Rev. Lett.* **2004**, 92, 146801.
- [7] R. G. Mani, J. H. Smet, K. von Klitzing, V. Narayanamurti, W. B. Johnson, V. Umansky, *Phys. Rev. B* **2004**, 69, 193304.
- [8] R. L. Willett, L. N. Pfeiffer, K. W. West, *Phys. Rev. Lett.* **2004**, 93, 026604.

- [9] R. G. Mani, *Physica E* **2004**, 22, 1.
- [10] J. H. Smet, B. Gorshunov, C. Jiang, L. Pfeiffer, K. West, V. Umansky, M. Dressel, R. Meisels, F. Kuchar, K. von Klitzing, *Phys. Rev. Lett.* **2005**, 95, 118604.
- [11] Z. Q. Yuan, C. L. Yang, R. R. Du, L. N. Pfeiffer, K. W. West, *Phys. Rev. B* **2006**, 74, 075313.
- [12] R. G. Mani, W. B. Johnson, V. Umansky, V. Narayanamurti, K. Ploog, *Phys. Rev. B* **2009**, 79, 205320.
- [13] S. Wiedmann, G. M. Gusev, O. E. Raichev, A. K. Bakarov, J. C. Portal, *Phys. Rev. Lett.* **2010**, 105, 026804.
- [14] S. Wiedmann, G. M. Gusev, O. E. Raichev, A. K. Bakarov, J. C. Portal, *Phys. Rev. B* **2010**, 81, 085311.
- [15] D. Konstantinov, K. Kono, *Phys. Rev. Lett.* **2009**, 103, 266808.
- [16] S. I. Dorozhkin, L. Pfeiffer, K. West, K. von Klitzing, J. H. Smet, *Nat. Phys.* **2011**, 7, 336.
- [17] R. G. Mani, C. Gerl, S. Schmult, W. Wegscheider, V. Umansky, *Phys. Rev. B* **2010**, 81, 125320.
- [18] R. G. Mani, A. N. Ramanayaka, W. Wegscheider, *Phys. Rev. B* **2011**, 84, 085308.
- [19] J. Iñarrea, R. G. Mani, W. Wegscheider, *Phys. Rev.* **2010**, 82, 205321.
- [20] R. G. Mani, *Int. J. Mod. Phys. B* **2004**, 1825, 3473189.
- [21] T. Ye, H.-C. Liu, W. Wegscheider, R. G. Mani, *Phys. Rev. B* **2014**, 89, 155307.
- [22] T. Y. Ye, H. C. Liu, Z. Wang, W. Wegscheider, R. G. Mani, *Sci. Rep.* **2015**, 5, 14880.
- [23] J. Iñarrea, G. Platero, *Phys. Rev. Lett.* **2005**, 94, 016806.
- [24] J. Iñarrea, G. Platero, *Phys. Rev. B* **2005**, 72, 193414.
- [25] J. Iñarrea, *Appl. Phys. Lett.* **2012**, 100, 242103.
- [26] J. Iñarrea, G. Platero, *Phys. Rev. B* **2011**, 84, 075313.
- [27] J. Iñarrea, *Appl. Phys. Lett.* **2011**, 99, 232115.
- [28] A. C. Durst, S. Sachdev, N. Read, S. M. Girvin, *Phys. Rev. Lett.* **2003**, 91, 086803.
- [29] X. L. Lei, S. Y. Liu, *Phys. Rev. Lett.* **2003**, 91, 226805.
- [30] P. H. Rivera, P. A. Schulz, *Phys. Rev. B* **2004**, 70, 075314.
- [31] J. Iñarrea, G. Platero, *Phys. Rev. B* **2008**, 78, 193310.
- [32] J. Iñarrea, *Appl. Phys. Lett.* **2008**, 92, 192113.
- [33] J. Iñarrea, G. Platero, *Appl. Phys. Lett.* **2009**, 95, 162106.
- [34] J. Iñarrea, *Appl. Phys. Lett.* **2007**, 90, 262101.
- [35] J. Iñarrea, *J. Appl. Phys.* **2013**, 113, 183717.
- [36] J. Iñarrea, *Sci. Rep.* **2017**, 7, 13573.
- [37] J. Iñarrea, G. Platero, *Appl. Phys. Lett.* **2008**, 93, 062104.
- [38] J. Iñarrea, G. Platero, *Phys. Rev. B* **1995**, 51, 5244.
- [39] Y. M. Beltukov, M. I. Dyakonov, *Phys. Rev. Lett.* **2016**, 116, 176801.
- [40] K. S. Novoselov, A. K. Geim, S. V. Morozov, D. Jiang, Y. Zhang, S. V. Dubonos, I. V. Grigorieva, A. A. Firsov, *Science* **2004**, 306, 666.
- [41] R. G. Mani, A. Kriisa, R. Munasinghe, *Sci. Rep.* **2019**, 9, 7278.
- [42] E. Mönch, D. A. Bandurin, I. A. Dmitriev, I. Y. Phinney, I. Yahniuk, T. Taniguchi, K. Watanabe, P. Jarillo-Herrero, S. D. Ganichev, *Nano Lett.* **2020**, 20, 5943.
- [43] J. Iñarrea, G. Platero, *New J. Phys.* **2021**, 23, 063004.
- [44] B. Hunt, J. D. Sanchez-Yamagishi, A. F. Young, K. Watanabe, T. Taniguchi, P. Moon, M. Koshino, P. Jarillo-Herrero, R. C. Ashoori, *Science* **2013**, 340, 1427.
- [45] M. Kindermann, B. Uchoa, D. L. Miller, *Phys. Rev. B* **2012**, 93, 115415.
- [46] G. Giovannetti, P. A. Khomyakov, G. Brocks, P. J. Kelly, J. van den Brink, *Phys. Rev. B* **2007**, 76, 073103.
- [47] K. Zollner, M. Gmitra, J. Fabian, *Phys. Rev. B* **2019**, 99, 125151.
- [48] O. V. Kibis, K. Dini, I. V. Iorsh, I. A. Shelykh, *Phys. Rev. B* **2017**, 95, 125401.
- [49] A. Iurov, G. Gumbs, D. Huang, *Phys. Rev. B* **2019**, 99, 205135.
- [50] V. P. Gusynin, S. G. Sharapov, J. P. Carbotte, *Int. J. Mod. Phys. B* **2007**, 21, 4611.
- [51] V. P. Gusynin, S. G. Sharapov, *Phys. Rev. B* **2005**, 71, 125124.
- [52] M. Koshino, T. Ando, *Phys. Rev. B* **2010**, 81, 195431.
- [53] M. M. Grujic, M. Z. Tadic, F. M. Peeters, *Phys. Rev. B* **2014**, 90, 205408.
- [54] S. Titeica, *Ann. Phys.* **1935**, 414, 129.
- [55] a) V. I. Ryzhii, *Sov. Phys. Solid State* **1970**, 11, 2078; b) V. I. Ryzhii, R. A. Suris, B. S. Shchamkhalova, *Sov. Phys. Semicond.* **1986**, 20, 1299.
- [56] V. Ryzhii, R. Suris, *J. Phys.: Condens. Matter* **2003**, 15, 6855.
- [57] A. C. Durst, S. Sachdev, N. Read, S. M. Girvin, *Phys. Rev. Lett.* **2003**, 91, 086803.
- [58] J. Iñarrea, G. Platero, *Sci. Rep.* **2022**, 12, 5157.
- [59] S. Das Sarma, S. Adam, E. H. Hwang, E. Rossi, *Rev. Mod. Phys.* **2011**, 83, 407.
- [60] E. H. Hwang, S. Das Sarma, *Phys. Rev. B* **2008**, 77, 115449.
- [61] A. Principi, M. Carrega, M. B. Lundeberg, A. Woessner, F. H. L. Koppens, G. Vignale, M. Polini, *Phys. Rev. B* **2014**, 90, 165408.
- [62] J. Iñarrea, G. Platero, *Appl. Phys. Lett.* **2006**, 89, 172114.
- [63] E. H. Kerner, *Can. J. Phys.* **1958**, 36, 371.
- [64] K. Park, *Phys. Rev. B* **2004**, 69, 201301.
- [65] N. Miura, *Physics of Semiconductors in High Magnetic Fields*, Oxford University Press, Oxford **2008**.
- [66] J. Iñarrea, G. Platero, *J. Phys.: Condens. Matter* **2015**, 27, 415801.
- [67] B. K. Ridley, *Quantum Processes in Semiconductors*, 4th ed, Oxford University Press, Oxford **1993**.
- [68] T. Ando, A. Fowler, F. Stern, *Rev. Mod. Phys.* **1982**, 54, 437.
- [69] R. Quhe, J. Zheng, G. Luo, Q. Liu, R. Qin, J. Zhou, D. Yu, S. Nagase, W. N. Mei, Z. Gao, J. Lu, *NPG Asia Mater.* **2012**, 4, 6.